This article was downloaded by: [Renmin University of China]
On: 13 October 2013, At: 10:38
Publisher: Taylor & Francis
Informa Ltd Registered in England and Wales Registered Number: 1072954 Registered office: Mortimer House, 37-41 Mortimer Street, London W1T 3JH, UK

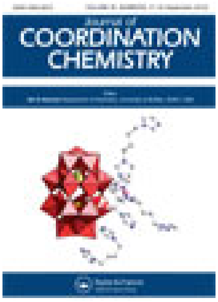

Journal of Coordination Chemistry
Publication details, including instructions for authors and subscription information:
http://www.tandfonline.com/loi/gcoo20

Construction of three 2-D silver(I) coordination architectures with a flexible pyrazine-based ligand

Jin'an Zhao [a] , Jiyong Hu [a] , Yun Bai [b] , Shufang Chen [b] & Shenshen Li [b]

[a] Department of Chemistry and Chemical Engineering , Henan University of Urban Construction , Henan 467036 , P.R. China

[b] Department of Chemistry , Zhengzhou University , Zhengzhou , Henan 450052 , P.R. China

Accepted author version posted online: 18 Jul 2012.Published online: 01 Aug 2012.

To cite this article: Jin'an Zhao , Jiyong Hu , Yun Bai , Shufang Chen & Shenshen Li (2012) Construction of three 2-D silver(I) coordination architectures with a flexible pyrazine-based ligand, Journal of Coordination Chemistry, 65:18, 3216-3226, DOI: 10.1080/00958972.2012.713103

To link to this article: http://dx.doi.org/10.1080/00958972.2012.713103

PLEASE SCROLL DOWN FOR ARTICLE

Taylor & Francis makes every effort to ensure the accuracy of all the information (the "Content") contained in the publications on our platform. However, Taylor & Francis, our agents, and our licensors make no representations or warranties whatsoever as to the accuracy, completeness, or suitability for any purpose of the Content. Any opinions and views expressed in this publication are the opinions and views of the authors, and are not the views of or endorsed by Taylor & Francis. The accuracy of the Content should not be relied upon and should be independently verified with primary sources of information. Taylor and Francis shall not be liable for any losses, actions, claims, proceedings, demands, costs, expenses, damages, and other liabilities whatsoever or howsoever caused arising directly or indirectly in connection with, in relation to or arising out of the use of the Content.

This article may be used for research, teaching, and private study purposes. Any substantial or systematic reproduction, redistribution, reselling, loan, sub-licensing, systematic supply, or distribution in any form to anyone is expressly forbidden. Terms &

Journal of Coordination Chemistry
Vol. 65, No. 18, 20 September 2012, 3216–3226

Construction of three 2-D silver(I) coordination architectures with a flexible pyrazine-based ligand

JIN'AN ZHAO*†, JIYONG HU†, YUN BAI‡, SHUFANG CHEN‡ and SHENSHEN LI‡

†Department of Chemistry and Chemical Engineering, Henan University of Urban Construction, Henan 467036, P.R. China
‡Department of Chemistry, Zhengzhou University, Zhengzhou, Henan 450052, P.R. China

(*Received 20 March 2012; in final form 12 June 2012*)

To investigate the impact of weak intermolecular interactions in construction of metal–organic frameworks, three silver(I) coordination complexes with the flexible N-heterocyclic ligand 1-((2-pyrazinyl)-1H-benzoimidazol-1-yl)methyl)-1H-benzotriazole (PBMBT), $\{Ag(C_{18}H_{13}N_7)NO_3\}_n$ (**1**), $\{Ag(C_{18}H_{13}N_7)ClO_4\}_n$ (**2**), and $\{Ag(C_{18}H_{13}N_7)SO_3CF_3\}_n$ (**3**), were prepared under solvothermal conditions and structurally characterized by single-crystal X-ray diffraction, IR spectrum, and elemental analyses. Complexes **1**–**3** exhibit 2-D reticulate structures, and these 2-D layers are further connected into 3-D supramolecular motifs by $\pi \cdots \pi$ interactions and hydrogen bonds. Luminescence indicates that **1**–**3** show analogous fluorescent emissions compared with the PBMBT in the solid state at room temperature.

Keywords: Metal–organic framework; Flexible ligands; Crystal structure; Photoluminescence properties

1. Introduction

Unlike traditional inorganic materials, metal–organic frameworks have attracted attention for intriguing structural features [1] and potential utilizations in magnetism [2], catalysis [3], luminescence [4], gas adsorption, [5] ion-exchange, etc. Factors causing different structures and properties of coordination polymers primarily depend on the metal ions and organic linkers with various configurations which offer different charge-balance requirements, alternative linking, and orientation of donors [6]. Thus, the key step in constructing coordination architectures is to employ suitable multidentate ligands as building blocks [7]. N-heterocycles including rigid ligands and flexible ligands have attracted attention, such as 2,4,6-tris(4-pyridyl)-1,3,5-triazine [8], 2-(pyridyl)benzimidazole [9], and 4,4′-bipyridine [10]. Rigid ligands have tiny or even no conformational changes when they react with metal salts. By contrast, flexible backbones can meet different coordination requirements of metal ions through changing their

---

*Corresponding author. Email: zjinan@zzu.edu.cn

Journal of Coordination Chemistry
ISSN 0095-8972 print/ISSN 1029-0389 online © 2012 Taylor & Francis
http://dx.doi.org/10.1080/00958972.2012.713103

conformations and may offer coordination architectures with unique structures and useful properties [11]; such ligands are di(1H-indazol-1-yl)methane [12], 1,3,5-tris(benzimidazol-1-ylmethyl)-2,4,6-trimethylbenzene) [13], 1,2-bis(1*H*-benzimidazol2-yl)-1,2-ethanol [14] and 2,3,5,6-tetrafluoro-1,4-5-(2-pyrazinyl)tetrazole-2-acetic acid [15].

Introduction of methylene $-CH_2-$ to an organic molecule can enhance its flexibility. The $-CH_2-$ supplies flexible orientation of a ligand arm and provides varied coordination generating more changes in the assembly process. Herein, 1-((2-pyrazinyl)-1H-benzoimidazol-1-yl)methyl)-1H-benzotriazole (PBMBT) was synthesized and reacted with Ag(I) salts. PBMBT not only has benzimidazole which possesses the specific proton accepting property and extensive $\pi\cdots\pi$ interactions, but also $-CH_2-$ that can freely bend and rotate to interact with metal centers [16]. Three new coordination complexes, $\{Ag(C_{18}H_{13}N_7)NO_3\}_n$ (**1**), $\{Ag(C_{18}H_{13}N_7)ClO_4\}_n$ (**2**), and $\{Ag(C_{18}H_{13}N_7)SO_3CF_3\}_n$ (**3**), based on PBMBT have been synthesized and structurally characterized. Luminescence measurements indicate that these complexes show analogous fluorescent emissions to PBMBT.

2. Experimental

2.1. *Materials and general methods*

Chemicals were purchased from commercial sources and used without purification. The 2-(2-pyrazine)-benzimidazole and PBMBT were synthesized according to the literature method [17]. IR spectra were recorded on a BRUKER TENSOR 27 spectrophotometer with KBr pellets from 400 to 4000 cm^{-1}. Elemental analyses (C, H, and N) were performed on a Flash EA 1112 elemental analyzer. X-ray powder diffraction (XRPD) data were measured on a PANalytical X'Pert PRO diffractometer using Cu-Kα1 radiation at room temperature. Thermogravimetric experiments were performed using a NETZSCH STA409 PC/PG thermal analysis instrument at a heating rate of 10°C min^{-1}, under a flux of nitrogen. Photoluminescence measurements were carried out using a spectrofluorimeter Hitachi F–4600 at ambient temperature in the solid state. The excitation and emission slit widths are both 2.5 nm, and the response time is 0.1 s.

2.2. *Synthesis of* $\{Ag(C_{18}H_{13}N_7)NO_3\}_n$ *(1)*

A mixture of $AgNO_3$ (0.0051 g, 0.03 mmol), PBMBT (0.0164 g, 0.05 mmol), and methanol (15 mL) was placed in a Teflon-lined stainless steel vessel. The mixture was sealed and heated at 100°C for three days, and then the reaction system was gradually cooled to room temperature at 5°C h^{-1}. Colorless rhombic block crystals were obtained. Yield: 56% (based on Ag). Elemental analysis Calcd for $AgC_{18}H_{13}N_8O_3$ (%): C, 43.48; H, 2.64; N, 22.54. Found: C, 43.42; H, 2.67; N, 22.49. IR(KBr/pellet, cm^{-1}): 3443.92(w), 3021.7(w), 1610.40(w), 1449.43(m), 1383.82(s), 1316.32(m), 1290.34(m), 1155.44(m), 1120.23(w) 1099.05(m), 1019.90(m), 755.63(s), 596.16(w).

2.3. *Synthesis of* $\{Ag(C_{18}H_{13}N_7)ClO_4\}_n$ *(2)*

A mixture of $AgClO_4$ (0.0113 g, 0.05 mmol), PBMBT (0.0164 g, 0.05 mmol), and methanol (15 mL) was placed in a Teflon-lined stainless steel vessel, the mixture was sealed and heated at 100°C for three days, and then the reaction system was gradually cooled to room temperature at $5^{\circ}C\,h^{-1}$. Colorless block crystals were obtained. Yield: 68% (based on Ag). Elemental analysis Calcd for $AgC_{18}H_{13}N_7ClO_4$ (%): C, 40.44; H, 2.45; N, 18.34. Found: C, 40.39; H, 2.40; N, 18.39. IR (KBr/pellet, cm^{-1}): 3446.69(w), 3030.64(w), 1610.08(w), 1536.87(w), 1494.93(w), 1450.84(s), 1397.71(s), 1298.62(m), 1170.85(s), 1103.42(s), 755.99(s), 623.13(s), 437.73(w).

2.4. *Synthesis of* $\{Ag(C_{18}H_{13}N_7)SO_3CF_3\}_n$ *(3)*

A mixture of $AgSO_3CF_3$ (0.0128 g, 0.05 mmol), PBMBT (0.0164 g, 0.05 mmol), and methanol (15 mL) was placed in a Teflon-lined stainless steel vessel, the mixture was sealed and heated at 100°C for three days, and then the reaction system was gradually cooled to room temperature at $5^{\circ}C\,h^{-1}$. Colorless block crystals were obtained. Yield: 45% (based on Ag). Elemental analysis Calcd for $AgC_{19}H_{13}N_7SO_3F_3$ (%): C, 39.06; H, 2.24; N, 16.78. Found: C, 39.12; H, 2.28; N, 16.70. IR(KBr/pellet, cm^{-1}): 3449.03(w), 3025.86(w), 2971.73(w), 1596.66(w), 1497.17(w), 1451.28(s), 1406.99(m), 1285.61(s), 1247.08(s), 1169.21(s), 1138.50(s), 1027.68(s), 758.78(s), 635.50(s), 516.14(m).

2.5. *Crystal structure determination*

A crystal suitable for X-ray determination was mounted on a glass fiber. Data of **1** were collected at room temperature on a Rigaku Saturn 724 CCD with graphite monochromated Mo-Kα radiation ($\lambda = 0.71073$ Å); data of **2** and **3** were collected at room temperature on a Gemini E with graphite monochromated Cu-Kα ($\lambda = 1.54184$ Å) radiation. The structures were solved by direct methods and expanded with Fourier techniques. The non-hydrogen atoms were refined anisotropically. Hydrogen atoms were included but not refined. The final cycle of full-matrix least-squares refinement was based on observed reflections and variable parameters. All calculations were performed with the SHELXL-97 crystallographic software package [18]. Crystal data and structure refinement details are provided in table 1 and selected bond distances and angles in table 2 for **1**–**3**.

3. Results and discussion

3.1. *Crystal structure of 1*

X-ray crystallographic data show that **1** crystallizes in the monoclinic space group $P21/c$. As shown in figure 1, the fundamental building unit is furnished by one Ag(I), one NO_3^-, and three PBMBT molecules. The distorted tetrahedral coordination sphere around each silver is built by O1, NO_3^-, and three nitrogen atoms (N1, N3a, and N7b) from pyrazine, benzimidazole, and benzotriazole groups of three PBMBT molecules. The Ag–O distance is 2.596 Å and the Ag–N distances vary from 2.246 Å to 2.313 Å;

Table 1. Crystal data and structure refinement for **1–3**.

Complex	**1**	**2**	**3**
Empirical formula	$C_{18}H_{13}AgN_8O_3$	$C_{18}H_{13}AgClN_7O_4$	$C_{19}H_{13}AgF_3N_7O_3S$
Formula weight	497.23	534.67	584.30
	293(2)	293(2)	293(2)
Wavelength (Mo-Kα) (Å)	0.71073		
Wavelength (Cu-Kα) (Å)		1.54184	1.54184
Crystal system	Monoclinic	Monoclinic	Monoclinic
Space group	$P21/c$	$P21/n$	$P21/c$
Unit cell dimensions (Å, °)			
a	11.453(2)	12.1863(7)	12.1197(4)
b	13.103(3)	12.3114(7)	12.6564(4)
c	15.760(5)	13.6740(9)	16.2351(8)
α	90	90	90
β	125.39(2)	103.059(7)	120.112(3)
γ	90	90	90
Volume (Å^3), Z	1928.1(8), 4	1998.5(2), 4	2154.25(14), 4
$F(000)$	992	1064	1160
θ range for data collection (°)	2.18–25.00	4.39–67.07	4.22–61.16
Final R_1^a, wR_1^b	0.0663, 0.1348	0.0486, 0.1421	0.0365, 0.0874
Goodness-of-fit on F^2	1.168	1.052	1.048

$^{a}R_1 = \sum||F_o| - |F_c||/\sum|F_o|$. $^{b}wR_2 = [\sum w(|F_o^2| - |F_c^2|)^2/\sum w|F_o^2|^2]^{1/2}$, $w = 1/[\sigma^2(F_o)^2 + 0.0297P^2 + 27.5680P]$, where $P = (F_o^2 + 2F_c^2)/3$.

Table 2. Selected bond lengths (Å) and angles (°) for **1**–**3**.

Complex **1**			
Ag(1)–N(3)#1	2.246(5)	Ag(1)–N(1)	2.273(5)
Ag(1)–N(7)#2	2.313(5)	Ag(1)–O(1)	2.596(7)
N(3)#1–Ag(1)–N(1)	132.48(18)	N(3)#1–Ag(1)–N(7)#2	107.15(17)
N(1)–Ag(1)–N(7)#2	106.14(18)	N(3)#1–Ag(1)–O(1)	93.5(2)
N(1)–Ag(1)–O(1)	118.2(2)	N(7)#2–Ag(1)–O(1)	91.96(19)
Complex **2**			
Ag(1)–N(5)#1	2.226(4)	Ag(1)–N(6)#2	2.242(4)
Ag(1)–N(1)	2.303(5)	N(6)#2–Ag(1)–N(1)	100.57(16)
N(5)#1–Ag(1)–N(6)#2	138.84(16)	N(5)#1–Ag(1)–N(1)	114.79(16)
Complex **3**			
Ag(1)–N(7)#1	2.239(4)	Ag(1)–N(5)	2.295(4)
Ag(1)–N(1)#2	2.294(3)	Ag(1)–O(3)	2.520(5)
N(7)#1–Ag(1)–N(5)	132.58(14)	N(7)#1–Ag(1)–N(1)#2	123.38(15)
N(5)–Ag(1)–N(1)#2	98.16(14)	N(7)#1–Ag(1)–O(3)	99.81(18)
N(5)–Ag(1)–O(3)	91.73(15)	N(1)#2–Ag(1)–O(3)	102.13(16)

Symmetry transformation used to generate equivalent atoms: #1 $-x+2$, $-y$, $-z+2$; #2 $x-1$, $-y-1/2$, $z-1/2$ for **1**; #1 $x+1/2$, $-y+1/2$, $z-1/2$; #2 $-x+3/2$, $y-1/2$, $-z+1/2$ for **2**; #1 $-x+1$, $-y$, $-z+2$; #2 $-x$, $y-1/2$, $-z+3/2$ for **3**.

similar bond lengths are observed in reported complexes [19]. As benzimidazole is more electron-rich than benzotriazole, the Ag–N distance (benzimidazole) [2.246 Å] is slightly shorter than that of Ag–N (benzotriazole) [2.313 Å]. Ag(I) centers are linked by PBMBT to form a 2-D structure with Ag···Ag separations of 5.225–7.940 Å (figure 2).

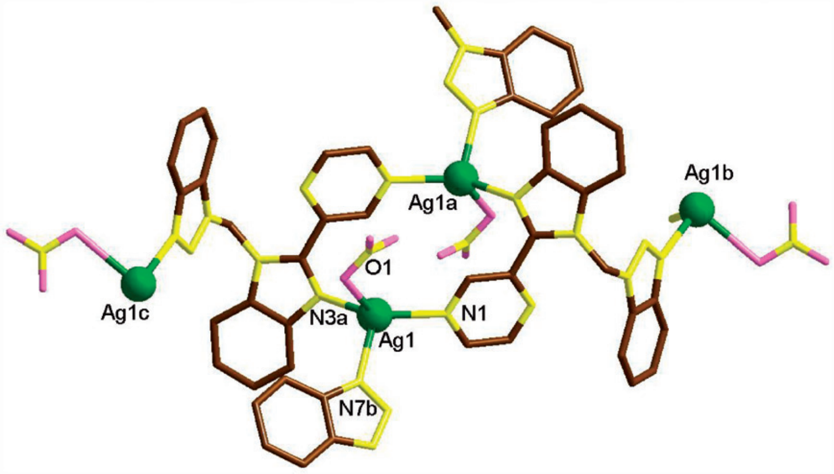

Figure 1. The coordination environment of Ag(I) in **1** (all hydrogen atoms are omitted for clarity).

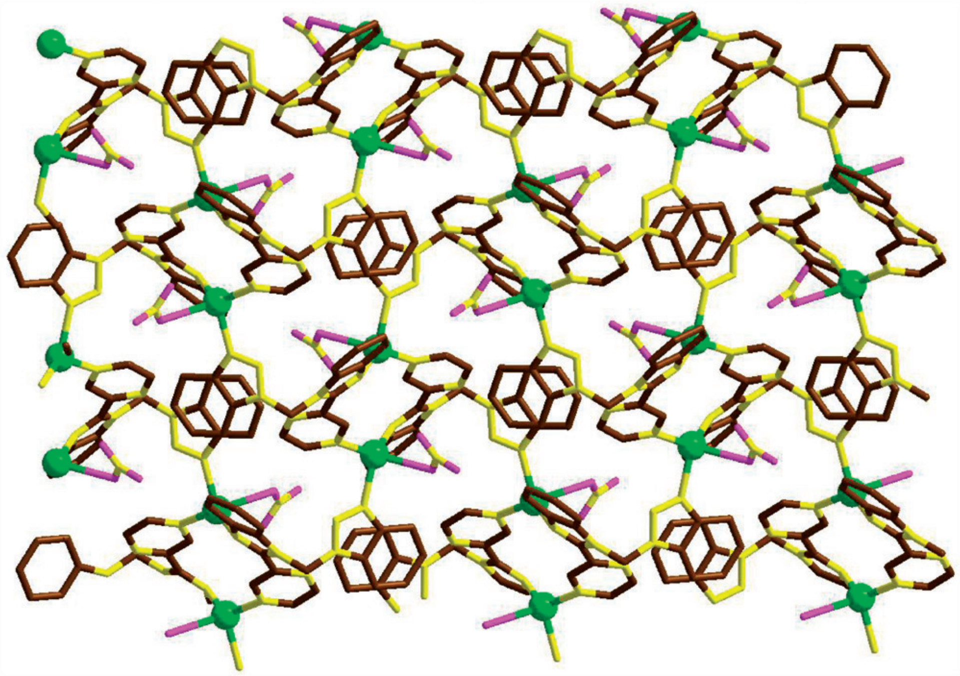

Figure 2. The 2-D structure of **1** (all hydrogen atoms are omitted for clarity).

Along the *b*-axis it can be seen that hydrogen bonds are present between carbons of PBMBT and oxygen atoms (C8–H8$\cdots$O2, 3.445 Å; C12–H12B$\cdots$O1, 3.235 Å; C12–H12B$\cdots$O2, 3.445 Å; C15–H15$\cdots$O2, 3.357 Å) which extend the 2-D layers into a 3-D supramolecular architecture. There also exist $\pi\cdots\pi$ interactions from aromatic

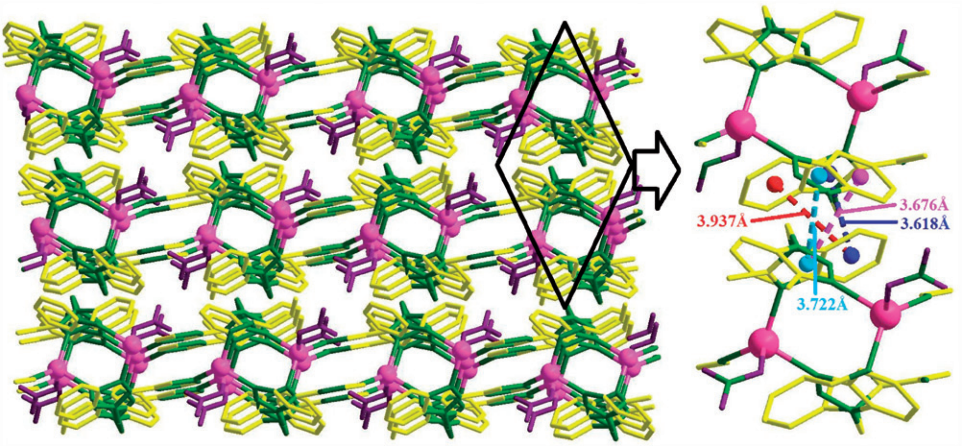

Figure 3. Packing diagram of 2-D layers of **1** viewed along the *b*-axis stabilized by hydrogen bonds and $\pi\cdots\pi$ interactions (all hydrogen atoms are omitted for clarity).

groups on neighboring layers with centroid distance of 3.618 Å (pyrazine ring to benzene ring with a dihedral angle of 1.45°), 3.676 Å (triazole ring to benzene ring with a dihedral angle of 1.02°), 3.722 Å (triazole ring to triazole ring with a dihedral angle of 0.02°), and 3.937 Å (benzene ring to benzene ring with a dihedral angle of 0°). H-bonding and $\pi\cdots\pi$ interaction play an important role in the formation and stability of **1** (figure 3).

PBMBT as a triply bridging ligand coordinates to Ag(I) by three nitrogen atoms, which stem from the pyrazinyl ring and benzimidazole group and benzotriazole moiety. In contrast, three complexes, $[Cd(Hpbi)Cl_2]$, $[Cd(Hpbi)_2Br_2]$, and $[Cd(Hpbi)_2I_2]$, were reported based on the rigid ligand 2-(pyrazin-2-yl)-1H-benzimidazole (Hpbi). The first one is 1-D "zigzag" chain and others are binuclear and mononuclear structures exhibiting 3-D supramolecular architectures through hydrogen bonds and $\pi\cdots\pi$ stacking interactions [20].

3.2. *Crystal structure of 2*

The substitution of $AgNO_3$ in **1** by $AgClO_4$ gives a 2-D motif **2**. As shown in figure 4, the fundamental building unit is composed of one Ag(I), one ClO_4^-, and three PBMBT molecules. Ag1a lies in a four-coordinate environment defined by O2 from ClO_4^- and N1, N5a, and N6b from benzimidazole, pyrazine, and benzotriazole of three PBMBT molecules. There are strong Ag···O contacts (Ag···O 2.715 Å) in **2**, similar to values reported for other silver(I) complexes [21]; Ag–N varies from 2.226 Å to 2.303 Å. Ag···Ag separations bridged by PBMBT are 5.133–8.146 Å (figure 5).

Hydrogen bonds are formed between carbon of each PBMBT and perchlorate (C5–H5···O3, 3.264 Å; C18–H18···O4, 3.487 Å) and these 2-D layers are further extended into a 3-D supramolecular architecture. There are also $\pi\cdots\pi$ stacking interactions with centroid distances of 3.753 Å (triazole ring to benzene ring with a dihedral angle of 1.25°), 3.766 Å (pyrazine ring to benzene ring with a dihedral angle

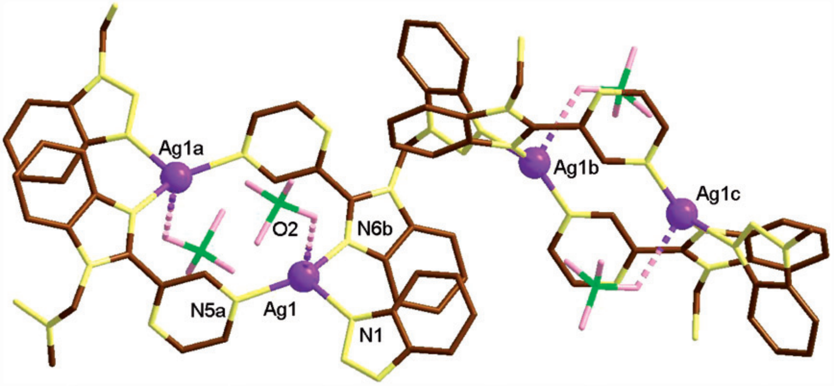

Figure 4. The coordination sphere of Ag(I) in **2** (all hydrogen atoms are omitted for clarity).

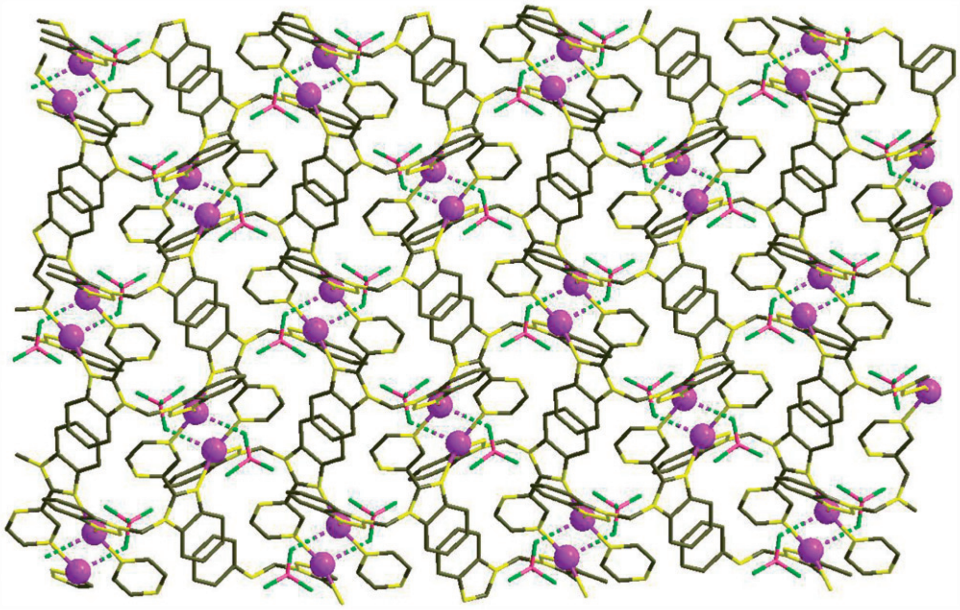

Figure 5. The 2-D structure of **2** (all hydrogen atoms are omitted for clarity).

of 0.41°), and 3.857 Å (triazole ring to triazole ring with a dihedral angle of 0°) in **2** (figure S1). The $\pi \cdots \pi$ stacking interactions and hydrogen bonds extend the structure into a 3-D supramolecular architecture. In contrast, the tridentate benzimidazole-based synthon dpa reacts with Cd(II) giving a 1-D double helical chain [Cd(dpa)(L1)], and these 1-D chains are further extended into 3-D supramolecular architecture by hydrogen bonds [22].

3.3. *Crystal structure of 3*

The replacement of $AgClO_4^-$ in **2** by $AgSO_3CF_3^-$ results in 2-D complex **3**, which also crystallizes in the monoclinic space group $P21/c$. As shown in figure 6, the asymmetric

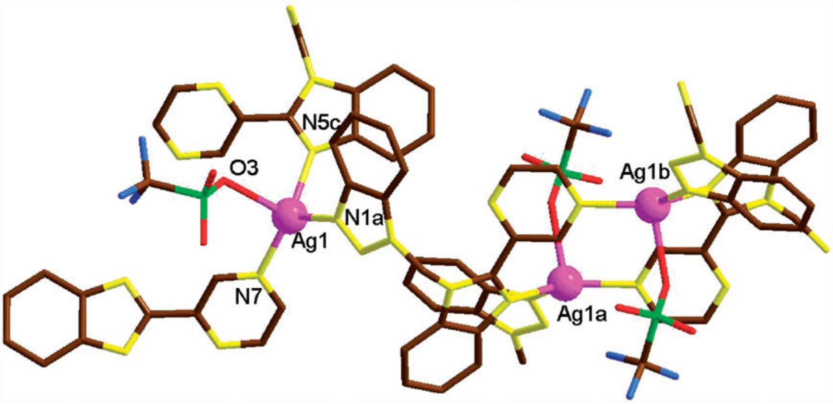

Figure 6. The coordination geometry of Ag(I) in **3** (all hydrogen atoms and solvent molecules are omitted for clarity).

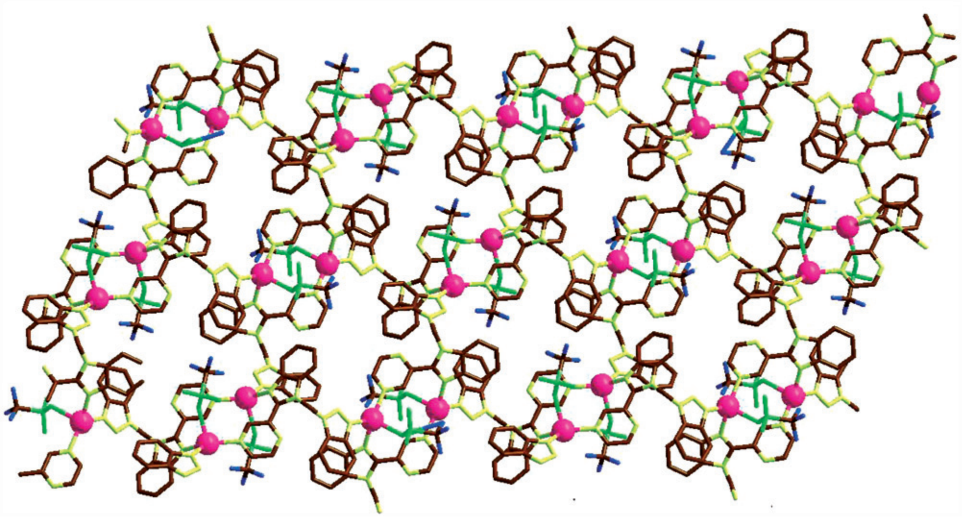

Figure 7. The 2-D structure of **3** (all hydrogen atoms are omitted for clarity).

unit of **3** consists of one Ag(I), one $SO_3CF_3^-$, and three PBMBT molecules. The Ag1 is a distorted tetrahedron defined by O3 from $SO_3CF_3^-$ group and three nitrogen atoms (N1a, N5c, and N7) from benzimidazole, pyrazine, and benzotriazole of three PBMBT molecules. The Ag–O distance is 2.520 Å, shorter than the ones in **1** and **2**, and Ag–N varies from 2.239 Å to 2.295 Å. Ag(I) centers are bridged to give a 2-D structure in which Ag···Ag distances are 5.272–8.724 Å (figure 7).

There are intermolecular hydrogen bonds between carbons of PBMBT and oxygen atoms (C2–H2···O2, 3.351 Å; C7–H7B···O2, 3.295 Å), and the 2-D layers are extended into a 3-D supramolecular architecture. Also, there are $\pi\cdots\pi$ interactions from neighboring layers with separations of 3.702 Å (triazole ring to benzene ring with a dihedral angle of 0.98°) and 3.930 Å (benzene ring to benzene ring with a dihedral angle of 0.02°) which also play crucial roles in stabilization of the 3-D structure (figure S2). In comparison, $[Zn(btaO)_2]_n$ and $[Cd(btaO)_2(H_2O)_4]\cdot 3H_2O$ based on a rigid ligand

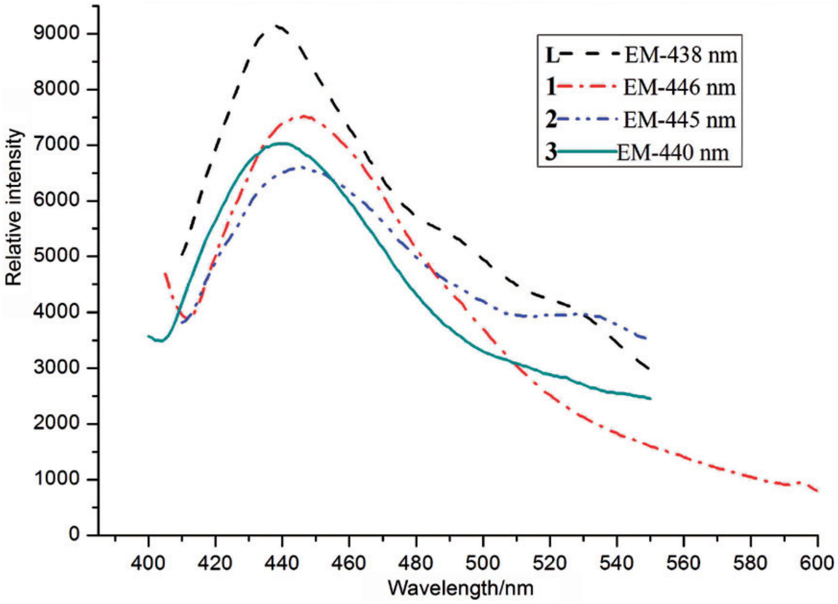

Figure 8. Photoluminescence spectra of **L** ($\lambda_{ex} = 398$ nm), **1** ($\lambda_{ex} = 396$ nm), **2** ($\lambda_{ex} = 394$ nm), and **3** ($\lambda_{ex} = 390$ nm) in the solid state at room temperature.

1-hydroxybenzotriazole (btaOH) bear double-stranded chains which are further supported by weak C–H···O hydrogen bonds resulting in a primitive cubic rod packing and a mononuclear structure, further connected to a 3-D supramolecular architecture by undulating hydrogen bonds, respectively [23].

3.4. *XRD and thermogravimetric analysis*

Complexes **1–3** are air-stable and retain their crystalline integrity at ambient temperature. PXRD patterns of **1–3** are essentially coincident with the simulated pattern derived from the single-crystal X-ray data, implying that the bulk sample is the same as the single crystal (figures S3–S5). Crystalline samples of **1** and **3** were subjected to thermogravimetric analysis under air to probe their thermal stabilities. As shown in figures S6 and S7, anhydrous **1** and **3** are thermally stable to 291.3°C and 276.4°C, respectively, and then lose weight. There are strong exothermic peaks at 296.1°C and 288.1°C for **1** and **3**, respectively, demonstrating decomposition. The differences between complex stabilities may be attributed to diverse interactions in the supramolecular motifs, which arise from distinct anions. The results imply that subtle differences of composition will lead to slightly different behaviors. Also, IR spectra (figures S8–S10) indicate the presence of the corresponding anions.

3.5. *Photoluminescence properties*

As illustrated in figure 8, **1–3** and PBMBT are luminescent in the solid state. At room temperature, PBMBT emits at 438 nm under excitation at 398 nm while **1–3** display relatively weak luminescence emissions at 446 nm ($\lambda_{ex} = 396$ nm), 445 nm ($\lambda_{ex} = 394$ nm), and 440 nm ($\lambda_{ex} = 390$ nm), respectively. Emission bands of PBMBT and **1**–**3** are similar in corresponding energy and band shape, so the emission bands are tentatively assigned as metal-perturbed π–π^* intraligand transitions [24]. The slight red shift of emission bands compared with PBMBT results from change of electron richness caused by introduction of metal. Fluorescence of **1**–**3** have been weakened slightly, which may be the heavy atom effect; silver can effectively enhance spin–orbit coupling and intersystem crossing efficiency, and therefore reduce the fluorescent emission [25].

4. Conclusion

Three new complexes based on PBMBT were synthesized under solvothermal conditions and characterized by single-crystal X-ray diffraction. Complexes **1**–**3** possess 2-D reticulate structures, with $\pi \cdots \pi$ interactions and hydrogen bonds playing crucial roles in formation and stabilization of these coordination networks. Luminescence measurements exhibit that **1**–**3** have fluorescent emissions similar to PBMBT.

Supplementary material

Crystallographic data for the structural analysis have been deposited with the Cambridge Crystallographic Data Center, CCDC reference numbers 856 931–856933. These data can be obtained free of charge *via* www.ccdc.cam.ac.uk/conts/retrieving.htm (or from the Cambridge Crystallographic Data Centre, 12 Union Road, Cambridge CB2 1EZ, UK; Fax: + 44 1223 336033).

Acknowledgments

We gratefully acknowledge the financial support by the Talent Supporting Plan of He'nan Scientific and Technological Innovation (No. 2010HASTIT016) and the He'nan key science and technology research (Nos 102102310079, 112102310084, and 122 102 310 061).

References

[1] (a) T.K. Maji, S. Sain, G. Mostafa, T.H. Lu, J. Ribas, M. Monfort, N.R. Chaudhuri. *Inorg. Chem.*, **42**, 709 (2003); (b) R. Wang, E. Gao, M. Hong, S. Gao, J. Luo, Z. Lin, L. Han, R. Cao. *Inorg. Chem.*, **42**, 5486 (2003); (c) S. Konar, P.S. Mukherjee, E. Zangrando, F. Lloret, N.R. Chaudhuri. *Angew. Chem. Int. Ed.*, **41**, 1561 (2002); (d) D. Feng, S.X. Liu, P. Sun, F.J. Ma, W. Zhang. *J. Coord. Chem.*, **63**, 1737 (2010).
[2] M. Kurmoo. *Chem. Soc. Rev.*, **38**, 1353 (2009).
[3] A. Corma, H. Garcia, F.X.L. Xamena. *Chem. Rev.*, **110**, 4606 (2010).
[4] M.D. Allendorf, C.A. Bauer, R.K. Bhakta, R.J.T. Houk. *Chem. Soc. Rev.*, **38**, 1330 (2009).

[5] W. Yang, A. Greenaway, X. Lin, R. Matsuda, A.J. Blake, C. Wilson, W. Lewis, P. Hubberstey, S. Kitagawa, N.R. Champness, M. Schröder. *J. Am. Chem. Soc.*, **132**, 14457 (2010).

[6] (a) Y.-B. Dong, Y.-Y. Jiang, J. Li, J.-P. Ma, F.-L. Liu, B. Tang, R.-Q. Huang, S.R. Batten. *J. Am. Chem. Soc.*, **129**, 4520 (2007); (b) A.B. Lysenko, E.V. Govor, H. Krautscheid, K.V. Domasevitch. *Dalton Trans.*, 3772 (2006).

[7] X. Lu, Y.Y. Chen, P.Z. Li, Y.G. Bi, C. Yu, X.D. Shi, Z.X. Chi. *J. Coord. Chem.*, **63**, 3923 (2010).

[8] M.X. Li, Z.X. Miao, M. Shao, S.W. Liang, S.R. Zhu. *Inorg. Chem.*, **47**, 4481 (2008).

[9] X.-P. Li, M. Pan, S.-R. Zheng, Y.-R. Liu, Q.-T. He, B.-S. Kang, C.-Y. Su. *Cryst. Growth Des.*, **7**, 2481 (2007).

[10] K.M. Blake, A. Banisafar, R.L. LaDuca. *Inorg. Chim. Acta*, **373**, 201 (2011).

[11] T. Ni, F. Xing, M. Shao, Y. Zhao, S. Zhu, M. Li. *Cryst. Growth Des.*, **11**, 2999 (2011).

[12] C. Pettinari, A. Marinelli, F. Marchetti, J. Ngoune, A. Galindo, E. Alvarez, M. Gomez. *Inorg. Chem.*, **49**, 10543 (2010).

[13] C.Y. Su, Y.P. Cai, C.L. Chen, F. Lissner, B.S. Kang, W. Kaim. *Angew. Chem. Int. Ed.*, **41**, 3371 (2002).

[14] Y.L. Zhou, F.Y. Meng, J. Zhang, M.H. Zeng, H. Liang. *Cryst. Growth Des.*, **9**, 1402 (2009).

[15] Q.-Y. Li, F. Zhou, C. Zhai, L. Shen, X.-Y. Tang, J. Yang, G.-W. Yang, Z.-F. Miao, J.-N. Jin, W. Shen. *Inorg. Chem. Commun.*, **14**, 843 (2011).

[16] Z. Pan, H. Zheng, T. Wang, Y. Song, Y. Li, Z. Guo, S.R. Batten. *Inorg. Chem.*, **47**, 9528 (2008).

[17] (a) A.W. Addison, P.J. Burke. *J. Heterocycl. Chem.*, **18**, 803 (1981); (b) A. Yoshimura, K. Nozaki, N. Ikeda, T. Ohno. *Bull. Chem. Soc. Japan*, **69**, 2791 (1996).

[18] (a) G.M. Sheldrick. *SHELXTL-97, Program for Crystal Structure Refinement*, University of Göttingen, Germany (1997); (b) G.M. Sheldrick. *SHELXS-97, Program for Crystal Structure Solution*, University of Göttingen, Germany (1997); (c) G.M. Sheldrick. *Acta Crystallogr., Sect. A*, **64**, 112 (2008).

[19] (a) H. Jiang, Y.Y. Liu, J.F. Ma, W.L. Zhang, J. Yang. *Polyhedron*, **27**, 2595 (2008); (b) C.Y. Li, C.S. Liu, J.R. Li, X.H. Bu. *Cryst. Growth Des.*, **7**, 286 (2007); (c) S.L. Zheng, A. Volkov, C. Nygren, P. Coppens. *Chem. Eur. J.*, **13**, 8583 (2007).

[20] Y.T. Wang, S.C. Yan, G.M. Tang, C. Zhao, T.D. Li, Y.Z. Cui. *Inorg. Chim. Acta*, **376**, 492 (2011).

[21] (a) M. Munakata, L.P. Wu, T. Kuroda-Sowa, M. Maekawa, Y. Suenaga, G.L. Ning, T. Kojima. *J. Am. Chem. Soc.*, **120**, 8610 (1998); (b) R.S. Zhou, J.F. Song, Y.B. Li, C.Y. Xu, X.F. Yang. *Z. Anorg. Allg. Chem.*, **637**, 251 (2011); (c) M.X. Li, Z.X. Miao, M. Shao, S.W. Liang, S.R. Zhu. *Inorg. Chem.*, **47**, 4481 (2008).

[22] L. Gou, L. Li, J.L. Li, X.Y. Fan, D.L. Li. *Z. Anorg. Allg. Chem.*, **636**, 1591 (2010).

[23] A.D. Katsenis, N. Lalioti, V. Bekiari, P. Lianos, C.P. Raptopoulou, A. Terzis, S.P. Perlepes, G.S. Papaefstathiou. *Inorg. Chem. Commun.*, **12**, 92 (2009).

[24] H. Chang, M. Fua, X.J. Zhao, E.C. Yang. *J. Coord. Chem.*, **63**, 3551 (2010).

[25] (a) X.H. Bu, W. Chen, W.F. Hou, M. Du, R.H. Zhang, F. Brisse. *Inorg. Chem.*, **41**, 3477 (2002); (b) X. Feng, J. Zhao, B. Liu, L. Wang, S. Ng, G. Zhang, J. Wang, X. Shi, Y. Liu. *Cryst. Growth Des.*, **10**, 1399 (2010).